

Supplementary Information

Controlling the lifetime of cucurbit[8]uril based self-abolishing nanozymes

Saurav Das, Tanushree Das, Priyam Das and Debapratim Das*

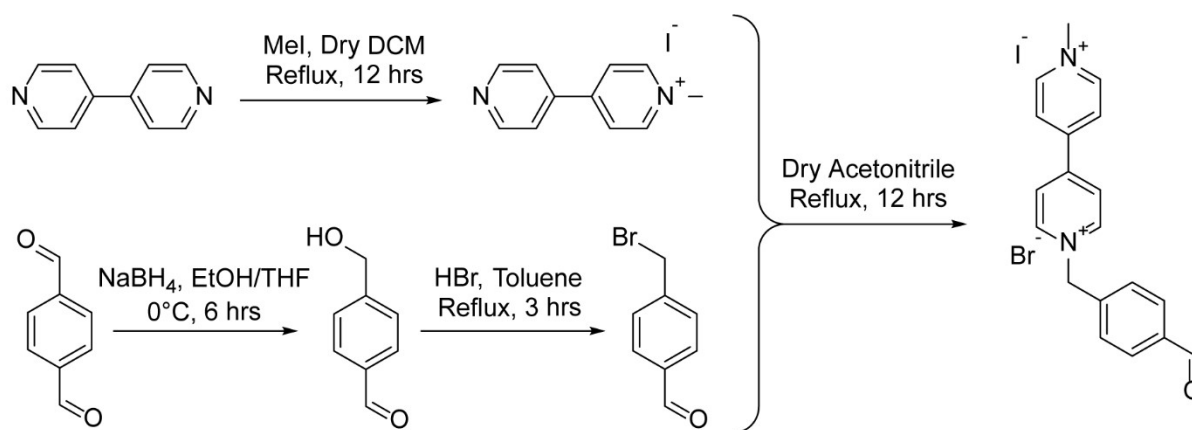
Department of Chemistry, Indian Institute of Technology Guwahati, North Guwahati,
Kamrup, Assam 781039, India

General Information and Materials:

2-Naphthaleneacetic acid, 4,4'-Bipyridyl, Methyl Iodide, 4-Nitrophenol, 2,4-Dinitrophenol, Triethylsilane (TES), 1,6-Diphenyl-1,3,5-hexatriene (DPH) and dodecylamine were purchased from Sigma-Aldrich (USA). Trifluoroacetic acid (TFA) were obtained from Spectrochem (India). Terephthalaldehyde, Chloroacetic acid were acquired from TCI Chemicals (India). Sodium Borohydride were procured from SRL (India). Cucurbit[8]uril (CB[8]) was synthesized following a previously published protocol¹ and characterized accordingly. Rink amide MBHA resin, protected amino acids and coupling reagents were purchased from Novabiochem. HPLC-grade dimethylformamide (DMF), dichloromethane (DCM) and acetonitrile (ACN) were procured from Spectrochem (India) and Fisher Scientific (India). Solvents were dried whenever required according to the reported procedures. Milli-Q water with a conductivity of less than $2 \mu\text{Scm}^{-1}$ was used for all sample preparations. 60-120 mesh silica gel (SRL) was used for column chromatography. Chromatographic purifications were performed on a Luna $5 \mu\text{m}$ (C18) column (Phenomenex) using a Dionex Ultimate 3000 HPLC. ^1H NMR and ^{13}C NMR spectra were recorded using a Bruker Ascend 600 MHz (Bruker, Coventry, UK) spectrometer and referenced to deuterated solvents. Coupling constants (J values) are reported in hertz, and chemical shifts are reported in parts per million (ppm). Multiplicities are reported as follows: s (singlet), d (doublet), t (triplet), m (multiplet), and br (broadened). Electrospray ionization mass spectrometry (ESI-MS) were performed with a Q-Tof-Micro Quadrupole mass spectrometer (Micromass) and data were analyzed using the built-in software.

Synthetic Procedures:

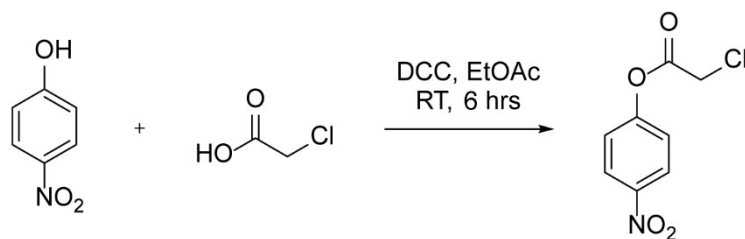
1-(4-formylbenzyl)-1'-methyl-[4,4'-bipyridine]-1,1'-dium (MV):



Scheme S1: Synthetic procedure of MV

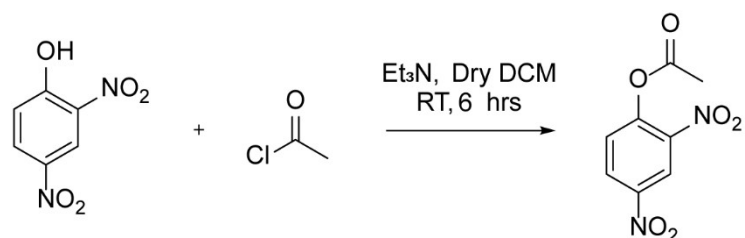
The aldehyde appended viologen derivative, **MV**, was synthesized following our previously reported protocol² and subsequently characterised.

4-nitrophenyl 2-chloroacetate (pNPCAA):



2-chloroacetic acid (500 mg, 5.291 mmols, 1 eqv.) and N,N'-dicyclohexylcarbodiimide (1.20 g, 5.82 mmols, 1.1 eqv.) was measured in a clean and dry 100 mL round bottom flask equipped with a magnetic stirrer. It was then sealed and purged with argon. To it 15 mL of dry EtOAc was added and then stirred at 0°C in an ice bath for 1 hour. To this continuously stirring reaction mixture a 10 mL solution of p-nitrophenol (810 mg, 5.822 mmols, 1.1 eqv.) dissolved in dry EtOAc was slowly added dropwise in the inert ice-cold condition. It was then allowed to stir at 0 °C for 1 hour and then gradually allowed to reach room temperature and stirred furthermore for 3 hours. The white precipitate obtained in the reaction mixture was discarded out by suction filtration. The reaction mixture was then concentrated by rotary evaporation to give a light-yellow sticky compound as the crude product. The crude product was purified by column chromatography over silica with an isocratic elution of 10% ethyl acetate in hexane to give a white crystalline solid compound as the pure product (462.02 mg, 40.5% yield). ¹H NMR (600 MHz, Chloroform-d) δ (ppm) 8.97 (d, *J* = 2.7 Hz, 1H), 8.53 (dd, *J* = 8.9, 2.7 Hz, 1H), 7.48 (d, *J* = 8.9 Hz, 1H), 2.43 (s, 3H).

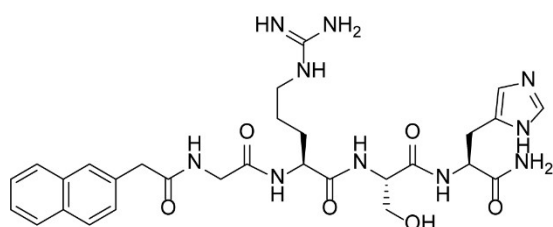
2,4-dinitrophenyl acetate (DNPA):



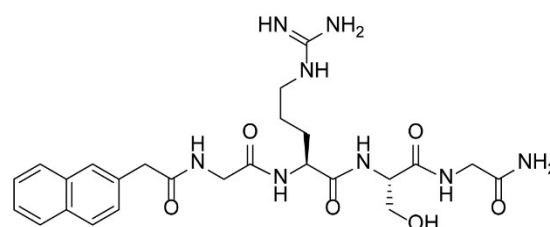
2,4-dinitrophenol (500 mg, 2.717 mmols, 1 eqv.) was measured in a clean and dry 100 mL round bottom flask equipped with a magnetic stirrer. It was then sealed and purged with argon. To it 10 mL of dry DCM was added and then stirred at 0°C in an ice bath. Triethyl amine (500 μL, 3.592 mmols, 1.32 eqv.) was then added dropwise under the continuously stirring inert condition at 0 °C which gave a clear yellow solution, which was then further allowed to stir for 30 minutes. To this continuously stirring cold reaction mixture, acetyl chloride (252 μL, 3.532 mmols, 1.30 eqv.) was slowly added dropwise. The reaction mixture was stirred for 1 hour in the inert ice-cold condition and then gradually allowed to reach room temperature, wherein it was further allowed to stir for 3 hours. A clear yellow reaction mixture was obtained which was then further diluted with 30 mL of dry DCM. This organic phase was then washed thrice with equal volumes of distilled water, once with brine and then collected and dried

over anhydrous Na₂SO₄. It was then filtered and concentrated by rotary evaporation to give the crude product as a clear yellow oily liquid. The crude product was then purified by column chromatography over neutral alumina with an isocratic elution in 15% ethyl acetate in hexane to give a white solid compound as the pure product. (371.9 mg, 60.5% yield). ¹H NMR (600 MHz, Chloroform-d) δ (ppm) 8.30 (d, *J* = 9.1 Hz, 1H), 7.35 (d, *J* = 9.1 Hz, 1H), 4.34 (s, 1H).

General Synthesis of the Peptide (Nap-His/Nap-Gly):



Nap-GRSH (Nap-His)



Nap-GRSG (Nap-Gly)

The peptides were synthesized on Rink amide MBHA resin using standard Fmoc (9-fluorenylmethoxycarbonyl) solid phase peptide synthesis (SPPS) protocol. In a typical coupling, 3 equiv. of protected amino acid (with respect to the loading of the resin), 3 equiv. of HBTU, and 6 equiv. of DIPEA were taken in 5 mL of DMF (for 0.1 mmol scale with respect to the resin loading) and stirred for 5 minutes prior to addition of the mixture to the swelled deprotected resin. The reaction mixture was shaken for 60 min and the resin was washed several times with DMF. The Fmoc-deprotection was achieved by treatment of the resin thrice with 5 ml of 20% piperidine in DMF for 5 minutes followed by thorough washing of the resin with DMF and DCM. The Fmoc-deprotection and coupling steps were repeated until the desired peptide sequence was obtained. The resin with the loaded peptide was washed several times with DMF and DCM and dried. The dried resin was then treated with a mixture of freshly prepared mixture of 8.5:1:0.5 (TFA/TES/H₂O) and stirred for 1 h. The resin was finally washed with DCM several times. The cleavage cocktail and the washings combined were concentrated to a minimum volume on a rotary evaporator. The cleaved peptide was then precipitated from cold dry ether, centrifuged and lyophilized to get the crude peptide. Purification was done in Dionex Ultimate 3000 HPLC using a Luna 5 μm (C18) column (Phenomenex) and using acetonitrile and water (containing 0.1% TFA each) as the mobile phase. (HPLC Program= 5% Acetonitrile/Water to 100% Acetonitrile in 25 minutes.)

Nap-His: ¹H NMR (600 MHz, DMSO-d₆) δ (ppm) 8.89 (s, 1H), 8.40 (t, *J* = 5.8 Hz, 1H), 8.18 (d, *J* = 8.3 Hz, 1H), 8.10 (dd, *J* = 21.8, 7.3 Hz, 1H), 7.86 (d, *J* = 7.7 Hz, 1H), 7.83 (d, *J* = 8.0 Hz, 2H), 7.74 (d, *J* = 18.5 Hz, 1H), 7.57 – 7.40 (m, 4H), 7.32 (d, *J* = 10.8 Hz, 3H), 4.46 (d, *J* = 5.0 Hz, 1H), 4.31 (d, *J* = 6.7 Hz, 1H), 4.21 (d, *J* = 6.3 Hz, 1H), 3.77 (d, *J* = 5.8 Hz, 2H), 3.64 (d, *J* = 16.3 Hz, 3H), 3.15 (dd, *J* = 15.4, 5.2 Hz, 1H), 3.06 (d, *J* = 7.4 Hz, 2H), 2.93 (dd, *J* = 15.5, 8.3 Hz, 1H), 1.67 (t, *J* = 6.1 Hz, 1H), 1.47 (dd, *J* = 13.8, 7.7 Hz, 3H). Mass (ESI-MS): *m/z* calcd. for C₃₅H₄₂N₉O₅⁺ [M+H]⁺: 624.308, found 624.081; C₃₅H₄₃N₉O₅²⁺ [M+2H]²⁺: 312.156, found 312.567; HPLC R_T = 9.25 min.

Nap-Gly: ^1H NMR (600 MHz, DMSO- d_6) δ (ppm) 8.39 (s, 1H), 8.11 (q, $J = 6.8, 6.3$ Hz, 3H), 7.91 – 7.81 (m, 3H), 7.77 (s, 1H), 7.52 – 7.40 (m, 3H), 7.32 – 7.11 (m, 5H), 4.36 (q, $J = 7.3$ Hz, 3H), 4.24 (q, $J = 6.3$ Hz, 2H), 3.75 (d, $J = 5.8$ Hz, 2H), 3.61 (d, $J = 15.8$ Hz, 3H), 3.13 – 2.99 (m, 4H), 1.68 (dd, $J = 15.1, 8.0$ Hz, 2H), 1.59 – 1.38 (m, 4H). Mass (ESI-MS): m/z calcd. for $\text{C}_{31}\text{H}_{38}\text{N}_7\text{O}_5^+$ $[\text{M}+\text{H}]^+$: 543.267, found 543.193; HPLC $R_T = 10.37$ min.

Experimental Methods:

UV-Visible and Fluorescence Spectroscopy: UV-Visible spectra were recorded on a PerkinElmer Lambda 750 spectrometer, while fluorescence measurements were performed on a Fluoromax 4 Plus spectrophotometer.

pH Measurements: The pH curves were recorded on a Hanna HI 2210 pH meter equipped with HI1131 pH probe from Hanna.

Field Emission Scanning Electron Microscopy (FESEM): 5 μL of the sample solution at specific time interval during the pH cycle was casted on a silicon wafer and immediately freeze-dried to arrest the kinetics of the pH cycle. FESEM imaging and Energy Dispersive X-ray (EDX) mapping analysis were then performed on a Gemini SEM 300 (Sigma Zeiss) instrument.

Field Emission Transmission Electron Microscopy (FETEM): 5 μL of the sample solution at specific time interval during the pH cycle was casted on carbon coated copper grid (300 mesh Cu grid with thick carbon film from Pacific Grid Tech, USA) and allowed to air dry for 2 minutes and then the excess sample was blotted with a tissue paper. The grid was then immediately freeze-dried and the FETEM images were taken in JEOL 2100F microscopes.

Isothermal Titration Calorimetry (ITC): ITC was performed using a Nano-ITC instrument from MicroCal for determining the formation constants and thermodynamic parameters for the inclusion complexes. 1 mM MV solution in buffer (10 mM phosphate, pH 7) was injected in parts (each injection, 1.3 μL) at an interval of 2 mins from a 40 μL micro-syringe into the Nap-His@CB[8] (1:1) solution (0.02 mM, 200 μL) with constant stirring (500 rpm) at 298K. All the solutions were degassed prior to titration. The ITC thermogram showed a 1:1 binding ratio between Nap-His@CB[8] and MV, thus indicating the formation of the ternary complex.

Preparation of CB[8] stabilized Host-Guest Ternary Complex:

To prepare 2 mL of 1 mM MV@CB[8] stock solution, 3.5 mg of CB[8] (the overall molecular weight of the used CB[8] was found to be 1730 from the elemental analysis data) and 1 mg of MV were accurately weighed into a 2 mL volumetric flask and 1.8 mL of MilliQ water was added to it. The heterogeneous solution was then sonicated for 1 hour at 298K. An equivalent amount of the peptide (Nap-His/Nap-Gly) was added to the solution of the binary complex, the volume was made up to 2 mL using MilliQ water and the solution was further sonicated for 1 hour at 298K. The light-yellow colored solution was then kept undisturbed at 298K for 1 day before utilizing for further experiments. The formation of the CB[8] stabilized charge-transfer ternary complex was confirmed by the appearance of a CT band at 394 nm and a significant drop in the fluorescence intensity of naphthalene. ITC experiment also confirmed the formation of the ternary complex.

Assessment of pH Dependent Hydrolase Activity:

Hydrolase activity of the vesicular nanozyme at pH 8 and 6, respectively, were assessed by spectrophotometrically monitoring the hydrolysis of p-nitrophenylacetate (pNPA) to p-nitrophenol (pNP). Briefly, 0.1 mM each of the TC (1 mM stock solution in water) and dodecylamine (10 mM stock solution in THF) were taken in 1 mL of pH 6 phosphate buffer (20 mM) or pH 8 TRIS buffer (20 mM) in a quartz cuvette of 1 cm path length and varying concentrations of pNPA (0.2, 0.4, 0.6, 0.8, 1.0 mM from 0.2 M stock solution in acetonitrile) were added to the solution. Following mixing, the absorbance changes corresponding to the chromogenic product, pNP were monitored at the pH independent isosbestic point for pNP, $\lambda_{\max} = 348 \text{ nm}$ ($\epsilon_{348\text{nm}} = 6.75 \text{ mM}^{-1} \cdot \text{cm}^{-1}$ in water) over a period of 5 minutes. The catalysis experiments were performed in triplicates and the kinetics of the reactions at different pH values were calculated via nonlinear regression using GraphPad Prism 9 software, under an assumption of Michaelis-Menten kinetics.

pH Gated Switching of Hydrolase Activity of the Nanozyme: The pH reversible nature of the nanozyme was assessed by alternatively switching the pH of an aqueous solution of the nanozyme (containing 0.1 mM each of TC and DA) between pH 6 and 8 using 0.01M HCl and NaOH, respectively. 1 mL aliquots of the solutions at different pHs were checked for hydrolase activity by treating with pNPA (0.5 mM) and monitoring the absorbance of the hydrolysed product, pNP at 348 nm. Disruption of the vesicular assembly at pH 6 led to a fall in the hydrolase activity of the nanozyme underpinning the critical role of the vesicular assembly in the catalysis reaction. Reconstitution of the nanozyme, however, restored the activity of the nanozyme over multiple cycles.

Programming of the pH Cycle:

Stock solutions of the activator, pH 9 TRIS buffer (1M), was prepared in MilliQ water and stored at 4°C for further use. For pH clock optimization, 1mL aqueous solution containing 0.1 mM each of the TC (1 mM stock solution in water) and dodecylamine (10 mM stock solution in THF), and the required amount of substrate (pNPA/pNPCAA/DNPA) was first acidified to a pH ~5 using 1mM HCl (to ensure disassembled state of the vesicles) and then the pH clock was initiated by addition of the required amount of pH 9 TRIS buffer. The change in pH was then monitored over time at 298K.

Time Dependent Dynamic Light Scattering (DLS) Studies: The particle sizes of the assemblies were obtained at 298 K using a 632.8 nm He–Ne laser using Zetasizer Nano-ZS90 (Malvern). Briefly, 1mL aqueous solution containing equimolar amounts (0.1 mM) of the TC (1 mM stock solution in water) and dodecylamine (10 mM stock solution in THF) was first acidified to a pH ~5 using 1mM HCl (to ensure disassembled state of the vesicles). The solution was filtered through appropriate filters to remove dust particles, if any, and the hydrodynamic size of the aggregates prior to the initiation of the pH clock (i.e., at 0 min) was found to be ~10nm. DLS measurements were performed immediately after the addition of the activator (1mM pH 9 TRIS buffer) and the substrate (5mM pNPCAA) and the hydrodynamic size distribution was monitored at specific time points at 298K. All measurements were performed with a constant angle of 90° and the results were reported as Number Distribution to reflect the number of aggregates formed. All measurements were performed in triplicates.

Fluorescence Kinetics Study for Transient Vesicle Formation:

Equimolar amounts (0.1 mM) of TC and dodecylamine along with 1 mM pNPCAA were dissolved together in MilliQ water and the pH of the solution was adjusted to ~5 prior to the initiation of the pH clock. 10 μM of the lipophilic dye, DPH (Diphenylhexatriene), was added to this solution and the initial fluorescence intensity was determined. The pH clock was then initiated by addition of pH 9 TRIS buffer (0.5 mM) and the emission intensity at 428 nm ($\lambda_{ex}=355$ nm, Slit width (Ex./Em.)= 5/5 nm) was monitored across three pH cycles over a period of 90 minutes.

Fluorescence Confocal Microscopy Studies: Transient nanozyme formation was performed as mentioned earlier but using Nile Red (10 μM) as the fluorescent probe as it specifically accumulates in the hydrophobic vesicle bilayer and shows fluorescence upon vesicle formation. Post initiation of the pH clock (1mM pH 9 TRIS buffer and 5mM pNPCAA), the assembly/disassembly process was monitored through CLSM wherein the transient vesicular nanozymes appeared as fluorescent aggregates and slowly disappeared as the nanozyme assemblies disassembled. The sample was excited at 488nm and the fluorescence emission was observed at 549 – 662 nm over a period of 60 min at 298K.

Particle Count Analysis from CLSM: The particle count from the CLSM images obtained at different time points were analyzed using ImageJ software. In particular, the images were converted to 8 bit

format and visible particles were counted. The particles having a minimum object dimension of 2, 4, 6, 8 and 10 px² were considered for particle count analysis. As anticipated, the number of fluorescent particles first increased upon initiation of the pH clock and then declined steadily as the pH clock concluded.

Supplementary Video Description: Transient formation of the vesicular nanozymes was visualized by monitoring the change in colour of the solution after the addition of the activator. In both the blank (water) and the nanozyme-containing solutions, alkaline buffer induced fast hydrolysis of the substrate (1mM pNPCAA), resulting in a yellow-coloured solution upon addition of the activator (0.5 mM pH 9 TRIS buffer). The colour of the nanozyme solution became transparent over a period of 80 minutes as a result of acidification of the medium by the acid produced by the nanozyme catalysed ester hydrolysis. The blank solution, on the other hand, stayed yellow, implying that there was no substantial reduction in pH. The shift in colour of the nanozyme containing solution from yellow to colourless suggested that the nanozymes had been disrupted at the end of the pH cycle.

Evidence for Cooperative mechanism for the hydrolase activity of the nanozyme:

As the pH sensitive nanozyme containing imine linked MV-DA tail group is highly susceptible to pH changes, in order to assess the catalytic mechanism of the nanozymes, a pH insensitive nanozyme containing HDMV as the tail group was synthesized. The pH insensitive nanozyme displayed a bell shaped curve for the pH dependent hydrolase activity with the maximum rate at pH 7 (close to the pK_a of histidine units). This pH dependent behaviour of the nanozyme is indicative of cooperative interaction amongst the neighbouring histidine units immobilized on the surface of the vesicular nanozyme.³ As a result of disruption of the pH sensitive nanozymes (MV-DA) at acidic pH, the cooperative effect is lost and protonation of the free histidine units (pK_a ~ 6) at acidic pH leads to the loss of catalytic activity of the dissociated nanozymes.

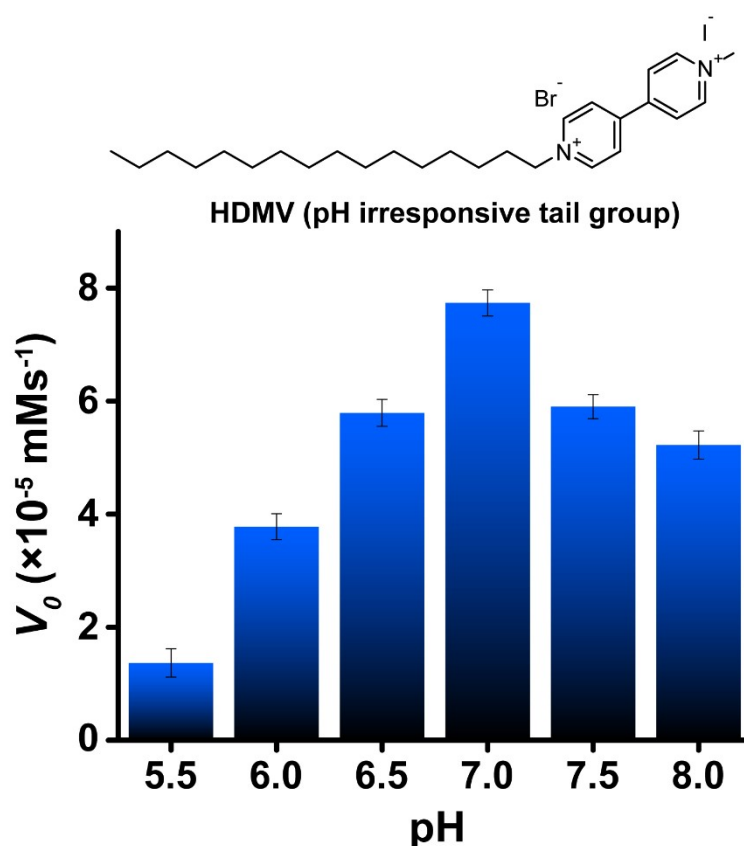


Fig. S1: Rate of hydrolysis of p-nitrophenyl acetate (pNPA) substrate using Nap-His head group and pH insensitive (Hexadecylmethylviologen, HDMV) tail group at different pH values. [CB[8]]/ [Nap-His]/ [HDMV]=100 μM , [pNPA]= 1mM.

HPLC Kinetics for the Hydrolysis of pNPCAA to pNP:

The hydrolysis of pNPCAA to pNP was monitored through Analytical High-Performance Liquid Chromatography (HPLC) using Dionex Ultimate 3000 HPLC system equipped with Luna 5 μm C18 column (Phenomenex) and using acetonitrile and water (containing 0.1% TFA each) as the mobile phase (HPLC Program= 0% Acetonitrile/Water to 100% Acetonitrile in 20 minutes). Briefly, 1 mL solution containing 0.1 mM each of the TC (1 mM stock solution in water) and dodecylamine (10 mM stock solution in THF) was prepared 1 mM pNPCAA was added to it. The pH of the solution was adjusted to ~ 5 and the hydrolysis reaction was initiated by adding 0.5 mM pH 9 TRIS buffer (1 M stock solution in water) to the solution. 50 μL aliquots of the solution were collected at specific time intervals and the reaction was quenched by acidifying the collected aliquots. The rate of hydrolysis was thereby monitored through HPLC at different time intervals and the amount of product formed was quantified using a standard plot prepared with known concentrations of pNP.

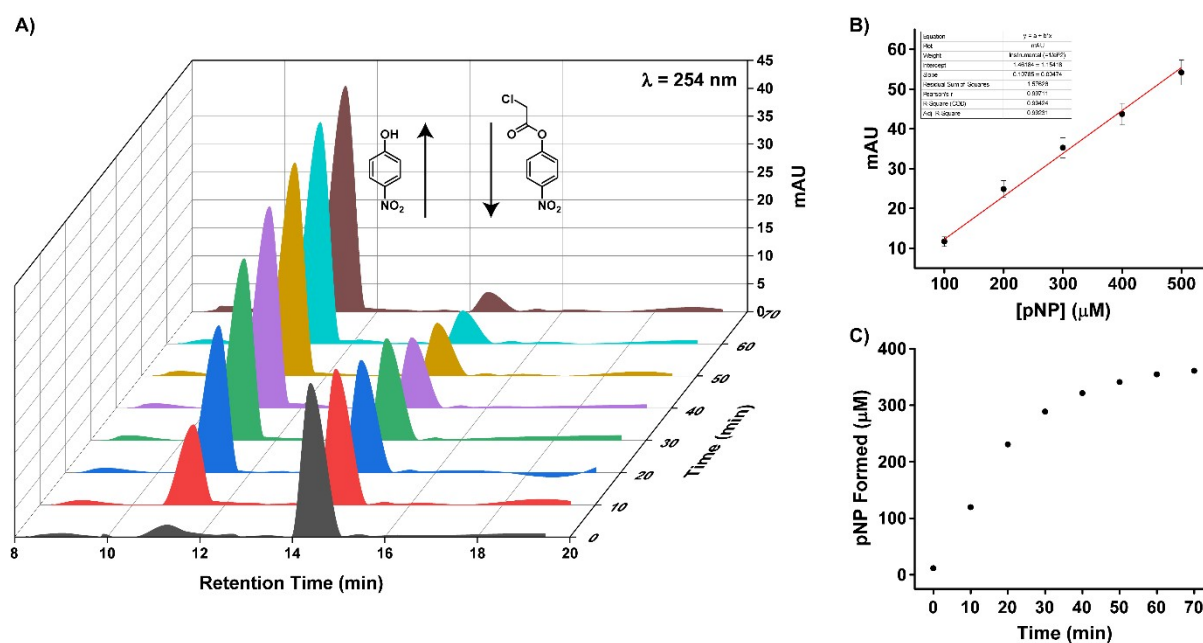


Fig. S2: (A) Time dependent HPLC chromatograms showing the nanozyme catalysed hydrolysis of pNPCAA to pNP, (B) Standard plot for pNP from HPLC, and (C) Time course generation of pNP from pNPCAA through the nanozyme catalysed ester hydrolysis reaction.

Time Dependent Fluorescence Kinetics Study:

DPH (Diphenylhexatriene) is a lipophilic probe that shows enhanced emission when entrapped in the hydrophobic nanodomains of vesicular assembly. The transient entrapment and resultant fluorescence enhancement of DPH (10 μM) was monitored at an interval of 1-minute post initiation of pH clock (0.5 mM pH 9 TRIS buffer, 1 mM pNPCAA). A rapid initial jump in emission intensity was followed by a gradual decay over a course of 90 minutes indicating the transient formation of the vesicular nanozymes.

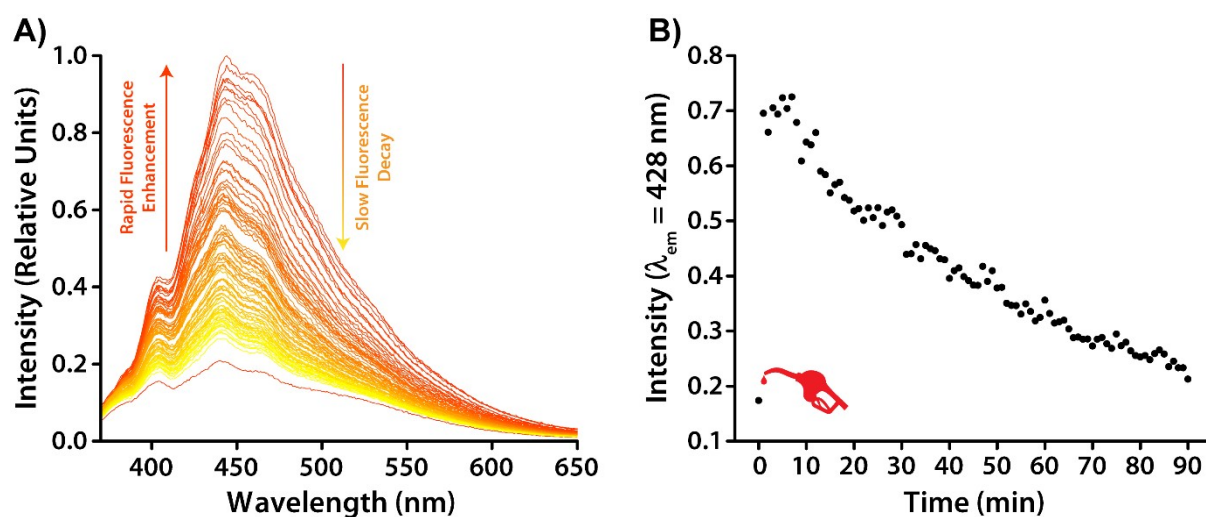


Fig. S3: (A) Time dependent emission spectra of DPH (10 μM) at different time intervals during the course of the pH cycle. [pH 9 TRIS Buffer]= 0.5 mM, [pNPCAA]= 1 mM. (B) Change in the emission intensity at $\lambda_{em} = 428 \text{ nm}$ ($\lambda_{ex}=355 \text{ nm}$, Slit width (Ex./Em.)= 5/5 nm) along the course of the pH cycle.

Particle Count Analysis:

Statistical analysis of the number of vesicles formed as observed in CLSM analysis showed emergence of fluorescence particles shortly after the initiation of the pH clock which slowly disappeared as the vesicles dissipated under the influence of the pH clock.

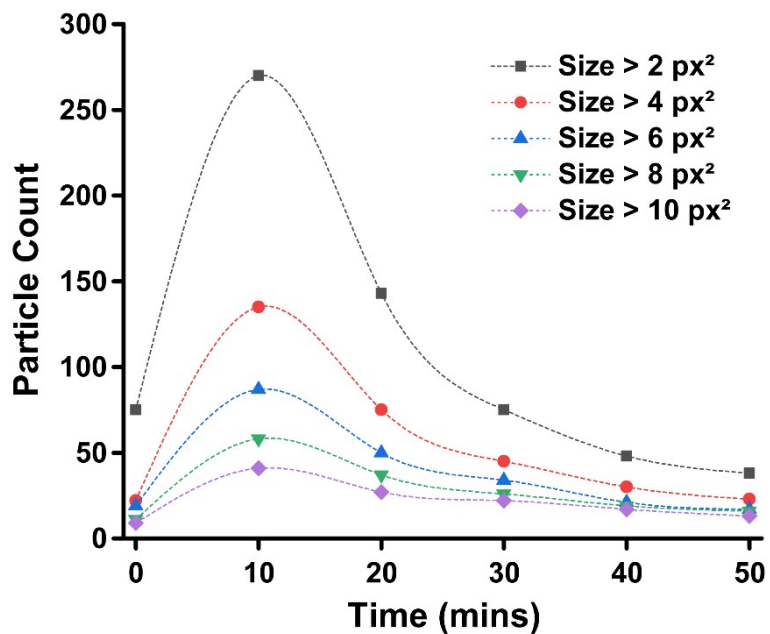


Fig. S4: Statistical analysis of the images obtained by confocal fluorescence microscopy.

Formation of pNP during the pH cycle:

Owing to considerable spectral overlap between the absorbance of the substrate, pNPCAA and the hydrolysed product, pNP, the time dependent kinetics for the hydrolysis of pNPCAA to pNP was monitored through HPLC. Briefly, 10 mL aqueous solution containing 0.1mM each of the **TC** and **DA**, along with 5 mM pNPCAA was initially maintained at pH ~5 and then subjected to the pH clock by addition of 1 mM pH 9 TRIS buffer. After the first pH cycle, only the activator (1mM pH 9 TRIS buffer) was added to initiate the second and third pH cycle. 50 μ L aliquots of the solution were collected at different time points and acidified to quench the catalysis reaction. The aliquots were subsequently subjected to chromatographic separation and the amount of pNP generated across three pH cycles was estimated using the calibration plot shown in Fig. S2B.

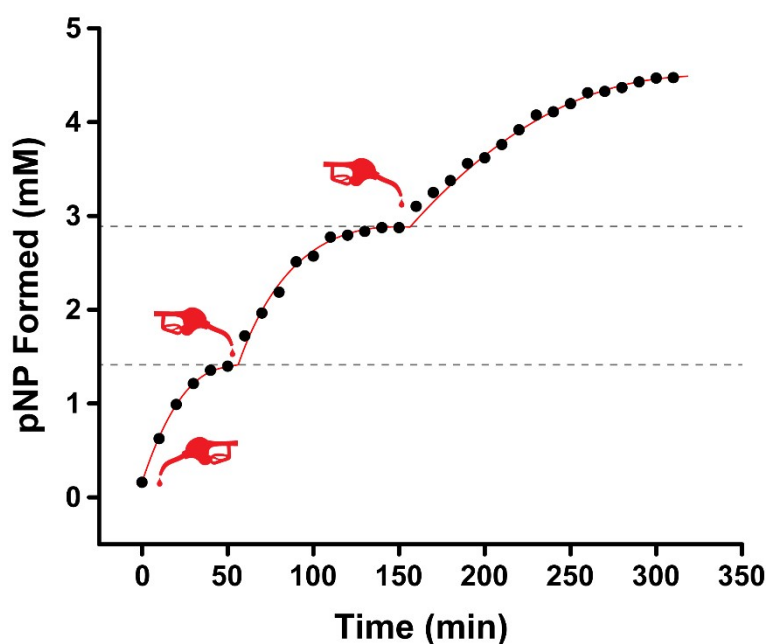


Fig. S5: Time dependent generation of pNP from pNPCAA by the nanozyme across three pH cycles as determined by HPLC measurements.

FESEM images of transient vesicles formed during the pH cycle (Figure 4C of the main manuscript):

Imine linkage between the aldehyde appended viologen (MV) unit of the TC and dodecylamine in pH 8 TRIS buffer was found to generate vesicles, which is in line with our previous observations.² To visualize the morphology of the assembled nanostructures at different time intervals during the course of the pH cycle, microscopic images of freeze dried samples of the nanozymes collected at specific time points were analysed using FESEM technique. The FESEM images showed no specific aggregation pattern before the initiation of the pH clock. However, upon addition of the activator, vesicles were observed as long as the pH of the solution was in the alkaline region. The vesicles, however, disappeared as the solution became acidic after 40 mins, indicating the transient nature of the vesicles.

Determination of Molar Extinction Coefficient of p-Nitrophenol/ 2,4-Dinitrophenol:

The molar extinction coefficient of pNP/DNP in water were determined by plotting the absorbance of known concentrations of pNP/DNPA in water at 348 nm and 355 nm, respectively. The slope of the linearly fitted concentration vs absorbance plot yielded the value $\epsilon_{348\text{nm}} = 6.75 \text{ mM}^{-1} \cdot \text{cm}^{-1}$ for pNP and $\epsilon_{355\text{nm}} = 9.62 \text{ mM}^{-1} \cdot \text{cm}^{-1}$ for DNP in water. All measurements were performed in triplicates.

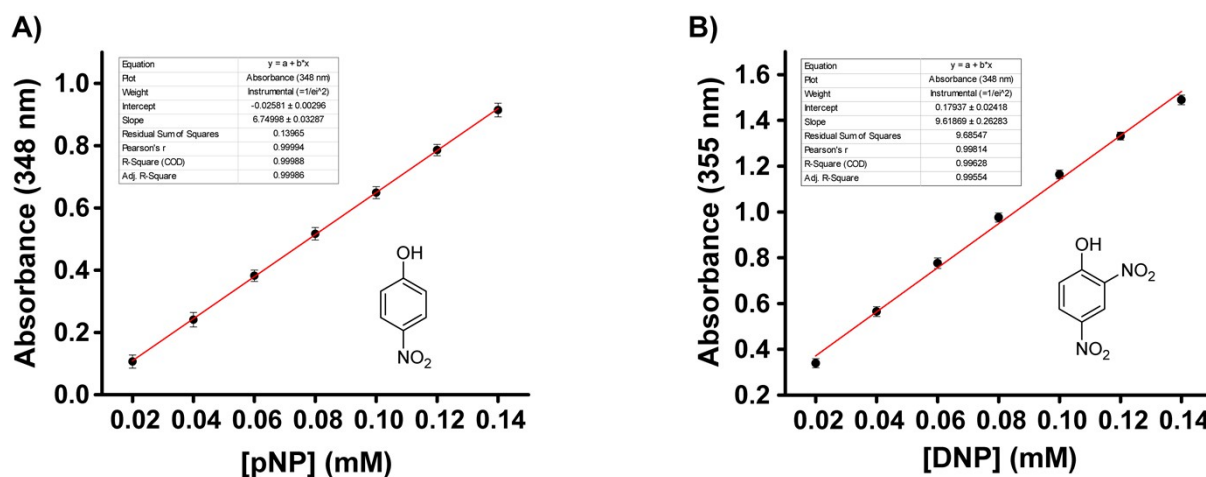


Fig. S6: Calibration plot for (A) p-nitrophenol and (B) 2,4-dinitrophenol in water.

Characterisation Data of the Synthesized Compounds:

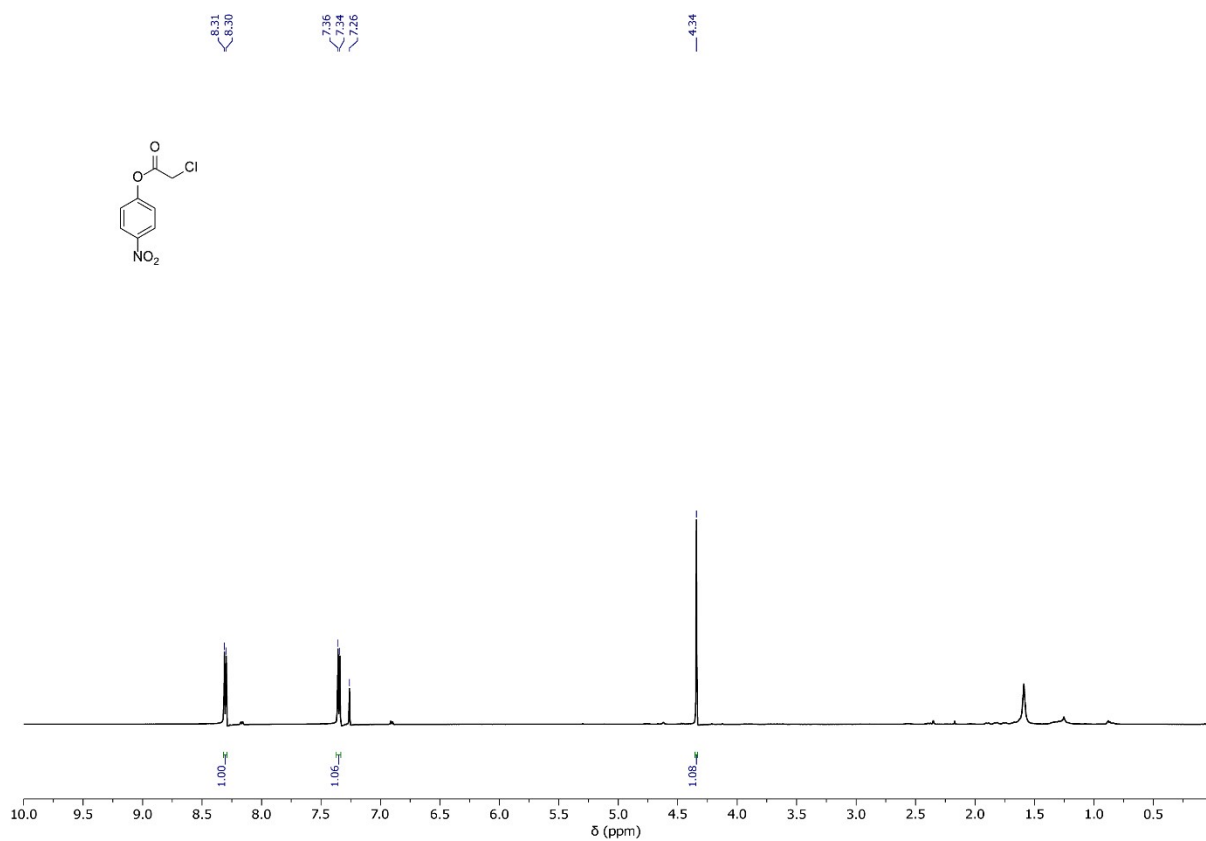


Fig. S7: ¹H NMR spectrum of pNPCAA in CDCl₃.

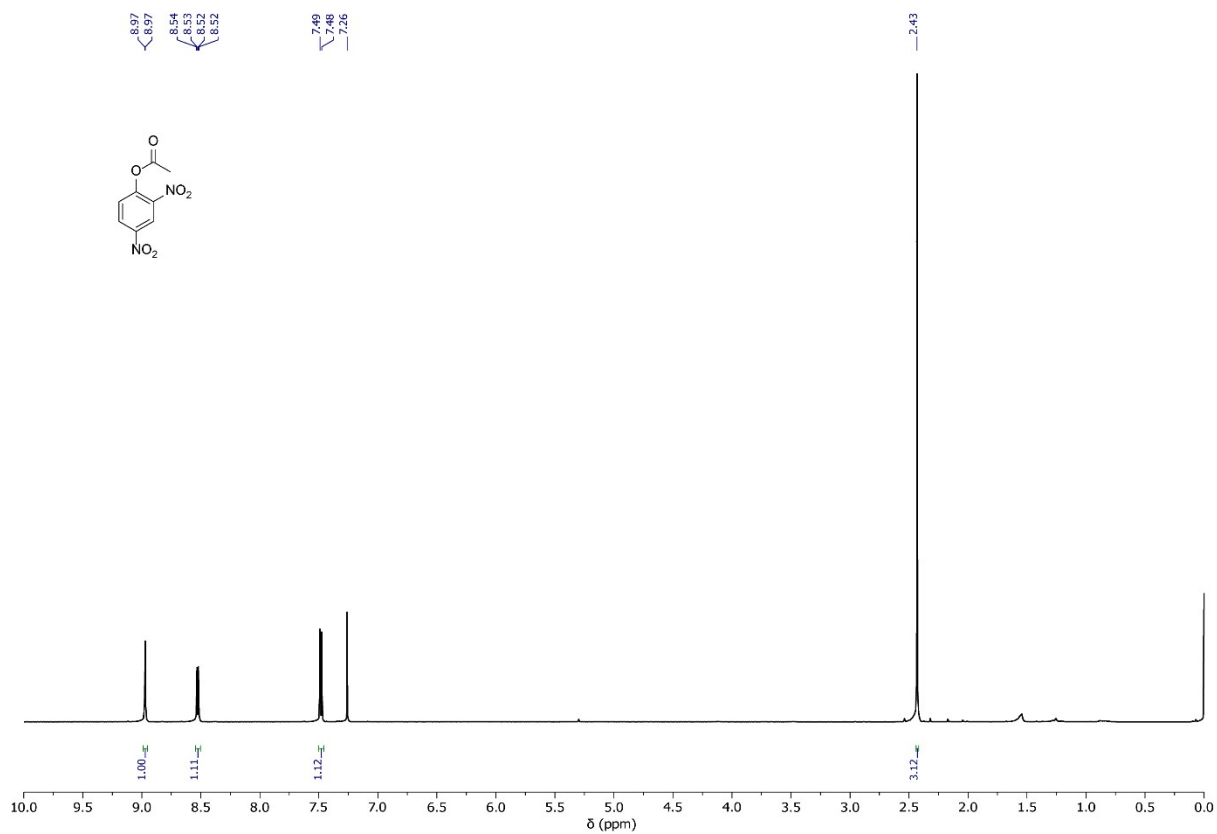


Fig. S8: ¹H NMR spectrum of DNPA in CDCl₃.

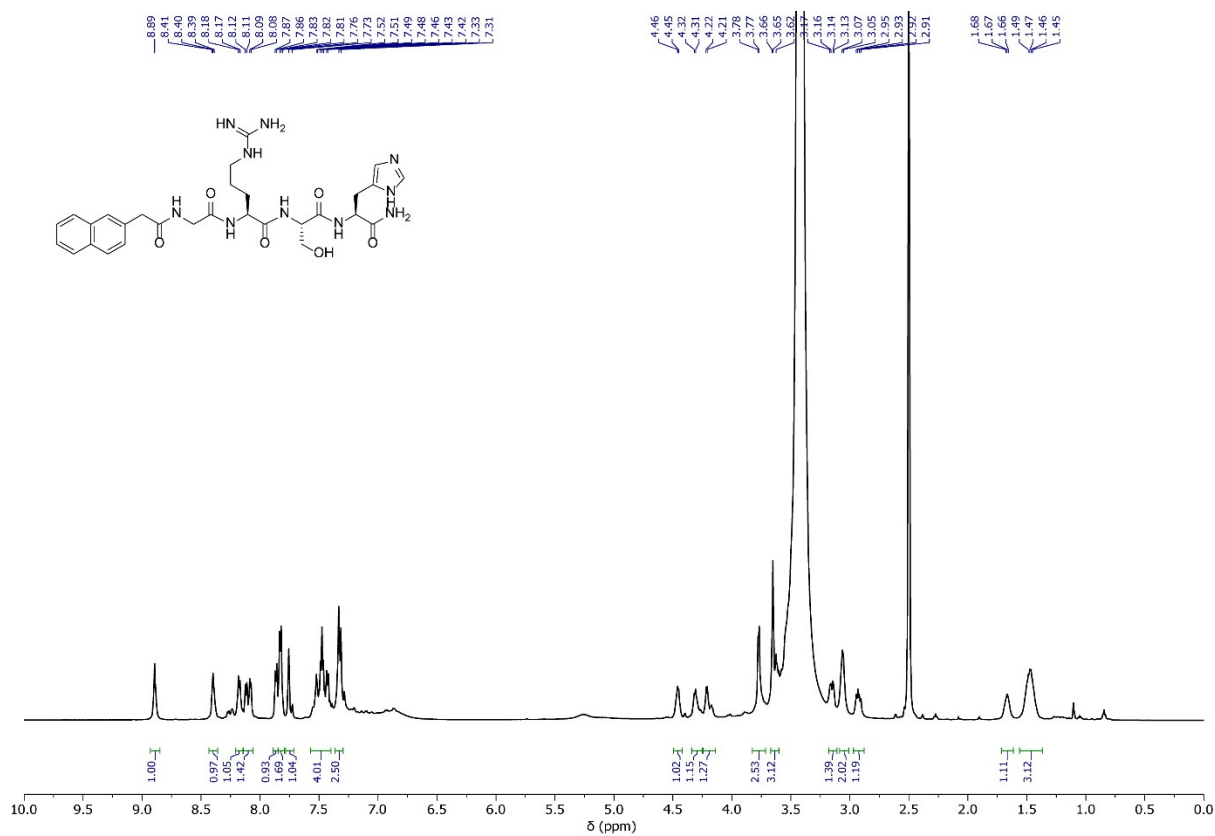


Fig. S9: ^1H NMR spectrum of Nap-His in DMSO-d_6 .

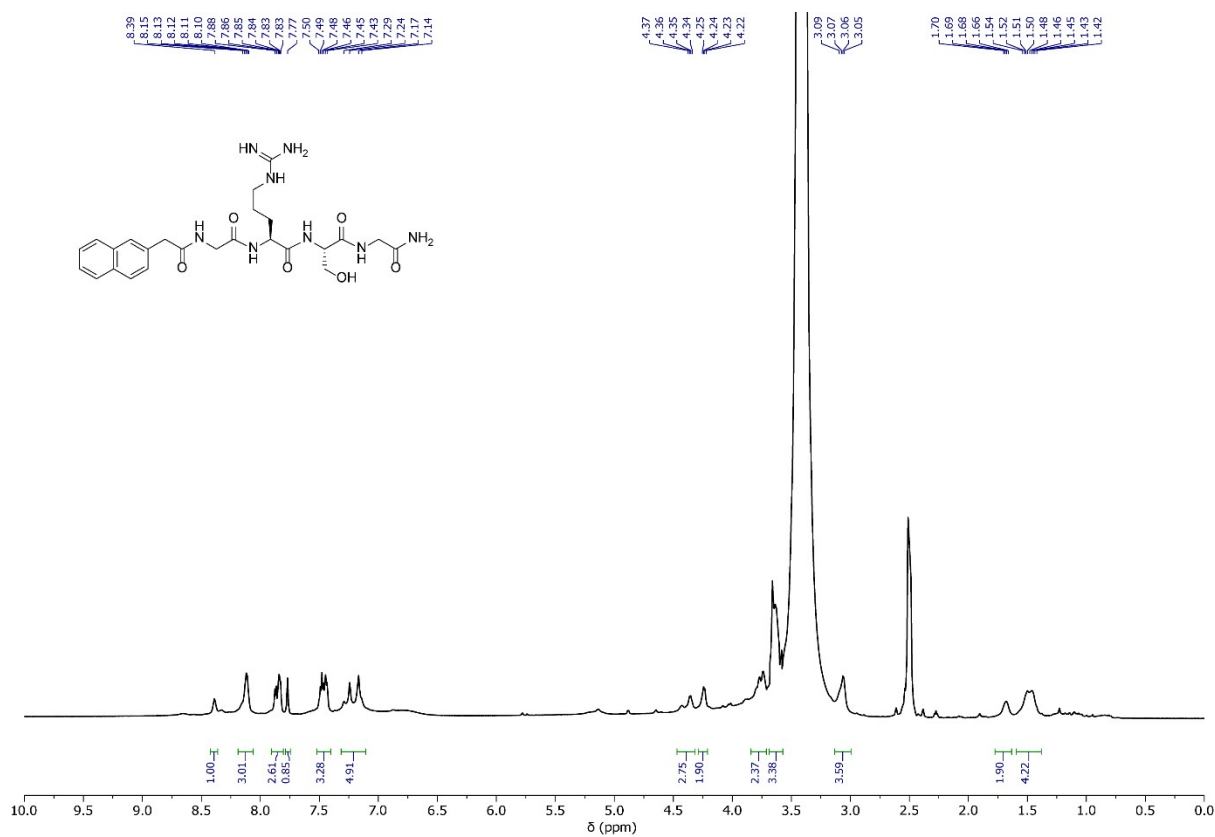


Fig. S10: ^1H NMR spectrum of Nap-Gly in DMSO-d_6 .

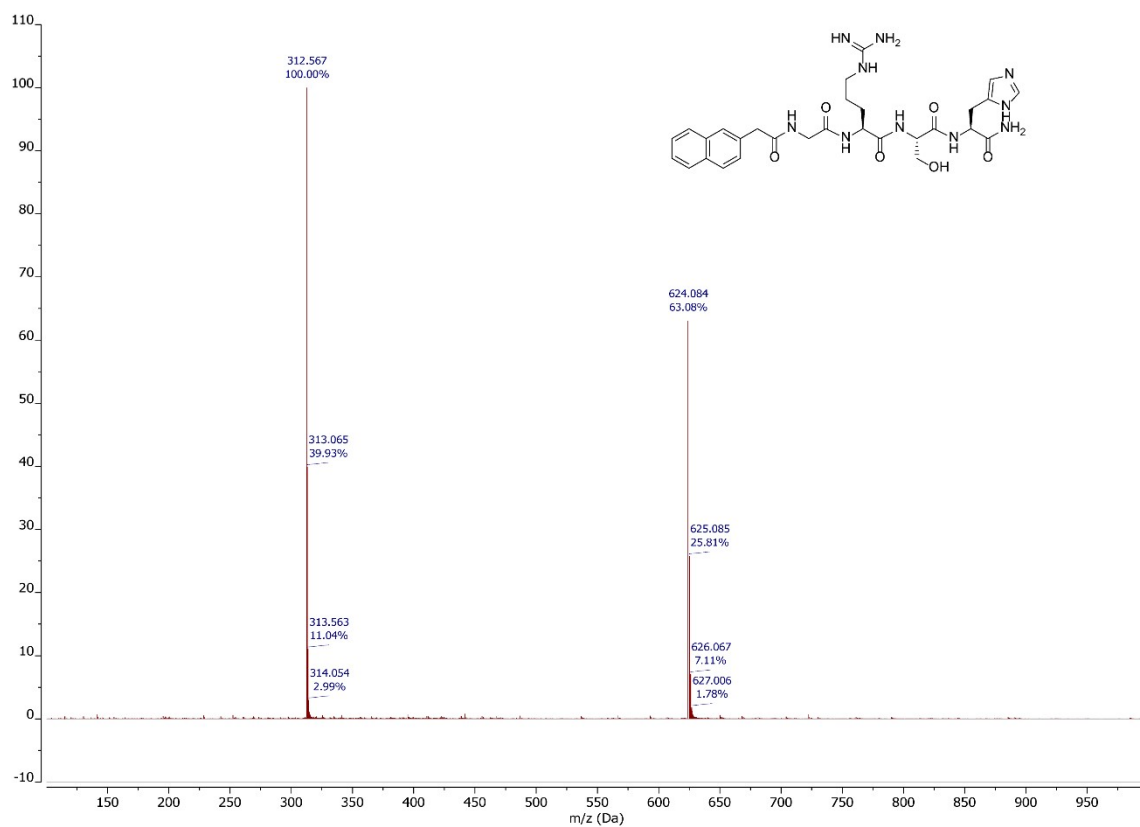


Fig. S11: ESI-MS of Nap-His.

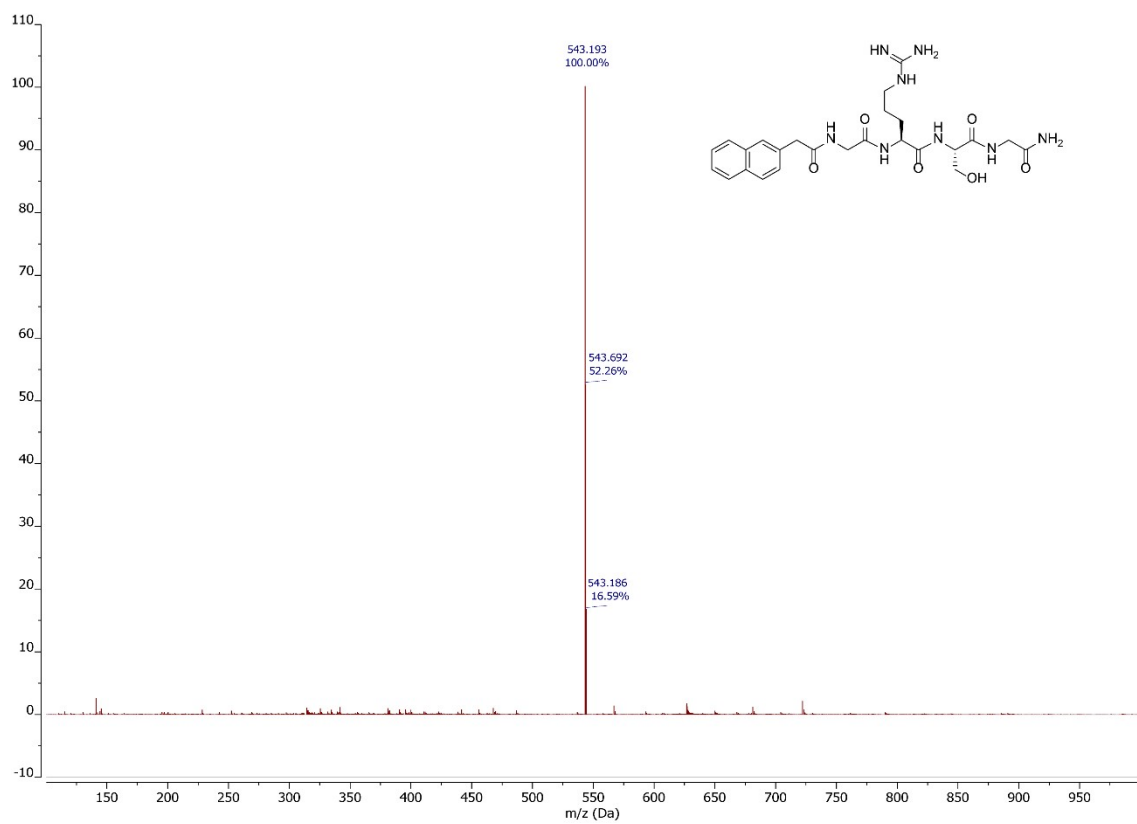


Fig. S12: ESI-MS of Nap-Gly.

References:

1. Kim, J.; Jung, I.-S.; Kim, S.-Y.; Lee, E.; Kang, J.-K.; Sakamoto, S.; Yamaguchi, K.; Kim, K., New Cucurbituril Homologues: Syntheses, Isolation, Characterization, and X-ray Crystal Structures of Cucurbit[n]uril (n = 5, 7, and 8). *J. Am. Chem. Soc.* **2000**, *122* (3), 540-541.
2. Dowari, P.; Das, S.; Pramanik, B.; Das, D., pH clock instructed transient supramolecular peptide amphiphile and its vesicular assembly. *Chem. Commun.* **2019**, *55* (94), 14119-14122.
3. Guarise, C.; Manea, F.; Zaupa, G.; Pasquato, L.; Prins, L. J.; Scrimin, P., Cooperative nanosystems. *J. Pept. Sci.* **2008**, *14* (2), 174-183.